

Triheterometallic lanthanide complexes made from kinetically inert lanthanide building blocks

Thomas Just Sørensen,^{*,[a, b]} Manuel Tropiano,^[b] Alan M. Kenwright,^[c] and Stephen Faulkner^{*,[b]}

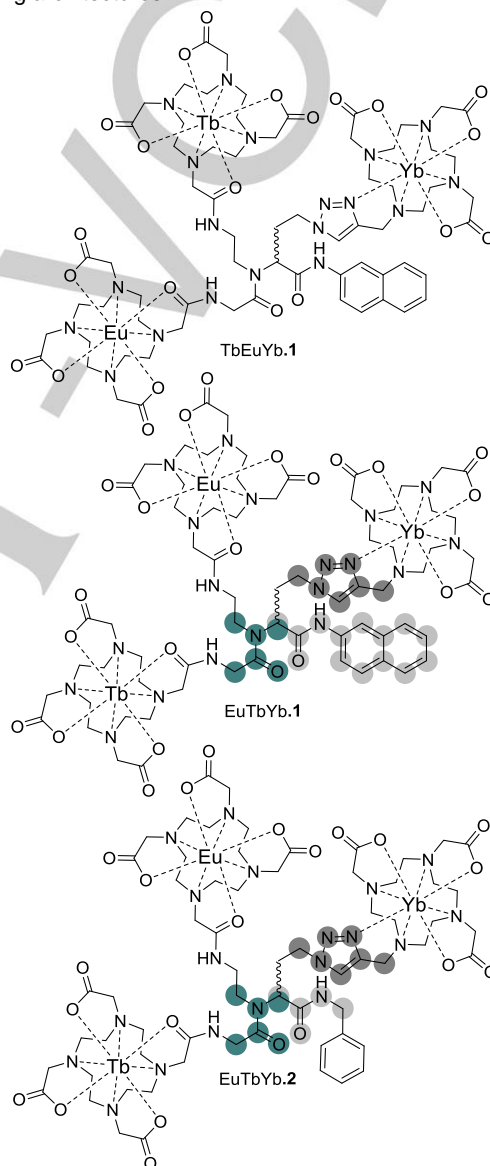
Abstract: Three molecular structures, each containing three different lanthanide(III) centres, were made by coupling three kinetically inert lanthanide(III) complexes in an Ugi reaction. These 2 kDa molecules were purified by dialysis, and characterised using NMR and luminescence. The photophysical properties of these heterotrimetallic complexes were investigated and are discussed by comparison with simpler, but related, heterobimetallic compounds. It was found that an amino-naphthalene unit inhibits sensitisation of terbium, while the spatial arrangement of the chromophores and lanthanide(III) centres in these molecules inhibited efficient sensitisation of europium. We conclude that the intramolecular collisions required for efficient Dexter energy transfer from the sensitizer to the lanthanide(III) centre can be prevented by steric congestion.

Introduction

Trivalent lanthanide ions play an important role in diagnostic magnetic resonance imaging and luminescent bioassay.^{1–6} To be useful in the clinic, the lanthanide(III) ion has to be incorporated in a kinetically inert complex, so no lanthanide(III) ions are released in the patient.^{2, 7–9} Multidentate ligands for lanthanide(III) ions based on a macrocyclic scaffold—typically 1,4,7-triazacyclononane (TACN) or 1,4,7,10-tetraazacyclododecane (cyclen)—has been used to form kinetically inert complexes.^{10–28} For cyclen, complexes with three and four monodentate pendant arms can be sufficient to form kinetically inert complexes, while TACN requires at least two bidentate pendant arms to form a kinetically inert complex with a trivalent lanthanide ion.

The kinetic stability of these complexes is of such a magnitude that heterometallic complexes can readily be made by using lanthanide(III) complexes as molecular building blocks. This approach has the merit of allowing highly defined systems to be prepared, obviating the problem of similarity between lanthanide(III) ions that effectively dooms any approach to specific (as opposed to merely selective) complexation under thermodynamic control. Kinetically inert lanthanide(III) complexes based on the 1,4,7,10-tetraazacyclododecane-1,4,7-

triacetic acid (DO3A) motif have been used in copper catalyzed azide alkyne click, diazotization, peptide coupling, and Ugi reactions to form multimetallic and heterometallic lanthanide(III) containing architectures.^{29–40}



Scheme 1. Trimetallic lanthanide(III) containing architectures investigated in this work.

In this manuscript, we demonstrate the use of the Ugi-coupling to make three heterotrimetallic lanthanide(III) containing architectures (Scheme 1), with three lanthanide(III) binding pockets covalently attached to a single tertiary amido nitrogen. By introducing small variations in the constitution of the architectures, it is possible to investigate the effect of solution structure on the properties of the systems, and we

- [a] Dr T. J. Sørensen
Nano-Science Center & Department of Chemistry
University of Copenhagen
Universitetsparken 5, 2100 København Ø, Denmark
E-mail: TJS@chem.ku.dk
- [b] Dr M. Tropiano, Dr Prof S. Faulkner
Chemistry Research Laboratory
Oxford University
12 Mansfield Road, Oxford OX1 3TA, UK
E-mail: Stephen.faulkner@keble.ox.ac.uk
- [c] Dr A. M. Kenwright
Department of Chemistry
Durham University
South Road, Durham DH1 3LE, UK

compare the properties of the three architectures in Scheme 1 to those of related heterobimetallic complexes we have recently studied.^{33, 34, 36, 40-42}

The actual structure of a lanthanide(III) complex in solution determines the magnetic and optical properties of the system as a whole.⁴³ For example the number of bound water molecules, q , is directly related to the relaxivity observed for a gadolinium based MRI contrast agent,¹ and a low q is very important when designing highly emissive lanthanide(III) complexes.⁴⁴ The solution structure of the lanthanide(III) complexes are difficult to address, since in just one symmetric binding pocket four coordination environments must be considered. Lanthanide(III) complexes of 1,4,7,10-tetraazacyclododecane-1,4,7,10-tetraacetic acid (DOTA) are found in solution as a mixture of four forms: a square antiprism (SAP), a twisted square antiprism (TSAP), a capped SAP (c-SAP), and a capped TSAP (c-TSAP). The choice of trivalent lanthanide ion, the solvent, and the presence of coordinating ions will affect the relative population of each form, while modifications in the ligand backbone might preclude the formation of one or more forms.^{1, 11, 16, 45-48} Furthermore, the nature of these structures defines the observed behaviour in a wide range of spectroscopic techniques: for open shell lanthanide(III) complexes, the overall structure of the lanthanide(III) complex (and the solvation sphere) determines the magnetic anisotropy at the metal, which in turn determines spectroscopic behaviour in NMR, EPR, and optical spectroscopy.^{43, 49-51}

In the compounds presented here (Scheme 1), the overall solution structure of the lanthanide architectures restricts binding of additional ligands at the lanthanide(III) centres and determines the outcome of the energy transfer cascades that result in sensitized emission from the lanthanide(III) centres. By investigating these properties in three highly crowded molecular structures containing a europium ion, a terbium ion, and an ytterbium ion in distinct binding pockets, we can explore the effect of solution structure. We have observed that we are able to block sensitization of a given lanthanide(III) ion by using steric bulk to limit the structure to the point where Dexter type energy transfer becomes essentially unfeasible, a finding that will be important in designing responsive heterometallic lanthanide(III) complexes for imaging and sensing. Our initial assumption that building condensed molecular structures with multiple functionalities would allow for multimodal sensors and probes was proven false, and we suggest that a more open design on a larger molecular backbone is needed to make larger functional architectures.

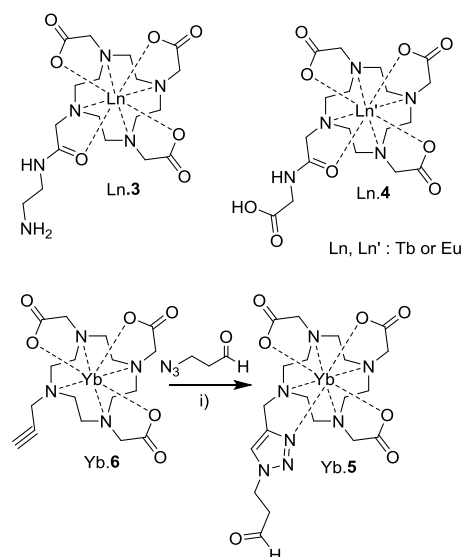
Results and Discussion

We have previously demonstrated the molecular building block approach to making large lanthanide(III) containing architectures.^{29, 30, 32, 33, 36, 37, 52-54} In this study, we used the three lanthanide(III) complexes Ln.3,⁵⁵ Ln.4,³⁴ and Yb.6 (shown in

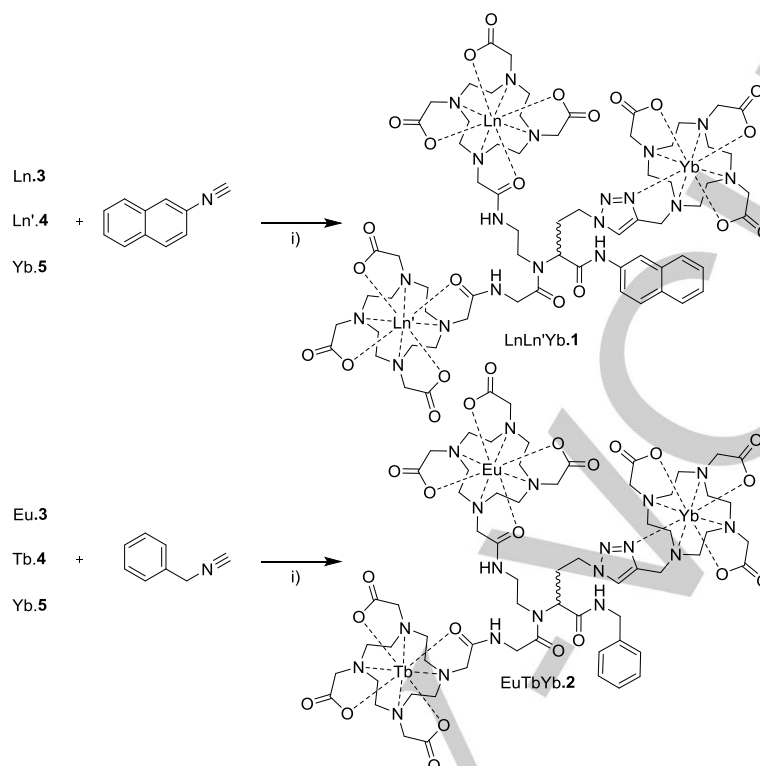
scheme 2) as building block.²⁹ The synthesis of the mononuclear lanthanide(III) complexes, the two DOTA monoamide complexes and the triazolyl-DO3A complex, was reported previously.^{29, 33, 34, 55} These building blocks contain an amine, a carboxylic acid, and a carboxaldehyde, which allow the coupling of all three in an Ugi reaction.

The three Ugi reactions shown in scheme 3 lead to the formation of the trinuclear triheterometallic lanthanide(III) complexes TbEuYb.1, EuTbYb.1, and EuTbYb.2. The complexes were purified by dialysis, and characterised using NMR and luminescence spectroscopy. Structures 1 and 2 differ in the isonitrile used in the Ugi coupling. Where 1 is formed by reaction with 2-naphthyl isonitrile, benzyl isonitrile was used for the preparation of 2. It is obvious that the photophysics of these chromophores are different, but is perhaps less obvious that the structural and electronic requirements imposed on the rest of the molecule by the choice of isonitrile is significantly different. In 1, there is a single sp^3 -hybridized carbon that may allow conformational freedom in the backbone, while the rest of the backbone is locked. In contrast, the structural restraint in 2 is only limited by two aliphatic amides, allowing for some degree of conformational freedom. The atoms that are should be in the same plane in favoured conformers are highlighted in Scheme 1. We have previously shown that the influence by remote substituents on backbones similar to the one in 1 and 2, may result in markedly different properties.^{34, 42}

Comparing molecular models of 1 and 2, the most pronounced difference lies in the fact that the naphthalene group can be completely excluded from the rest of the molecule (figure 1).



Scheme 2. Molecular building blocks used (i: Cu(I), TBTA, DCM / MeOH).



Scheme 3. Ugi coupling reaction producing the TbEuYb.1, EuTbYb.1, and EuTbYb.2 architectures (i: Na₂SO₄ in ethanol).

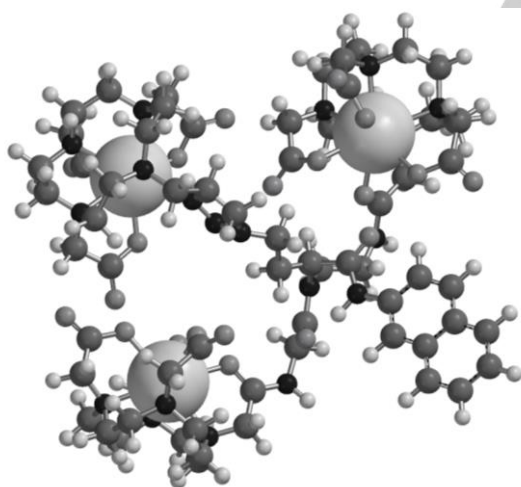


Figure 1. Molecular model of LnLn'Yb.1, Carbon = Grey, Hydrogen = White, Nitrogen = Black, Oxygen = Light grey, Ln = White (large).

These large lanthanide(III) containing architectures have proven particularly difficult to characterise. The materials are very hygroscopic, preventing elemental analysis, while mass spectrometry did not yield any data for TbEuYb.1, EuTbYb.1, or EuTbYb.2. The starting materials are readily identified using mass spectrometry, and it is a curiosity that the larger architectures cannot be found using a series of modern

ionisation techniques in combination with several different mass analysers.

NMR and luminescence proves the presence of the three different lanthanide(III) ions and lanthanide(III) binding pockets (and also demonstrates that the structures close to individual lanthanide(III) ions are significantly different to those of the complexes used as starting materials). Furthermore, the mass spectrometry results preclude the presence of the starting materials, supporting the presence of the target molecules.

EuTbYb.1 and EuTbYb.2 have the three lanthanide(III) ions in identical binding pockets, where europium and terbium in TbEuYb.1 have exchanged position. The NMR spectra of EuTbYb.1 and EuTbYb.2 are shown in Figures 2 and 3. The resonances corresponding to protons in the terbium and ytterbium binding pockets can be identified by cursory inspection. These resonances are found at similar shifts and with almost identical intensity in the two spectra. The spectrum in Figure 4 is markedly different to the spectra found in Figures 2 and 3. The resonances corresponding to protons on the terbium-binding pocket indicate that this part of the molecule exists in two different conformations. The corresponding resonances from the protons in the europium binding pockets of EuTbYb.1 and EuTbYb.2 are in the crowded region of the spectrum between 30 and -30 ppm. The Yb binding pocket shows fewer resonances in TbEuYb.1 or it may be that sharp lines from Tb are crowding that region in the spectra of EuTbYb.1 and EuTbYb.2.

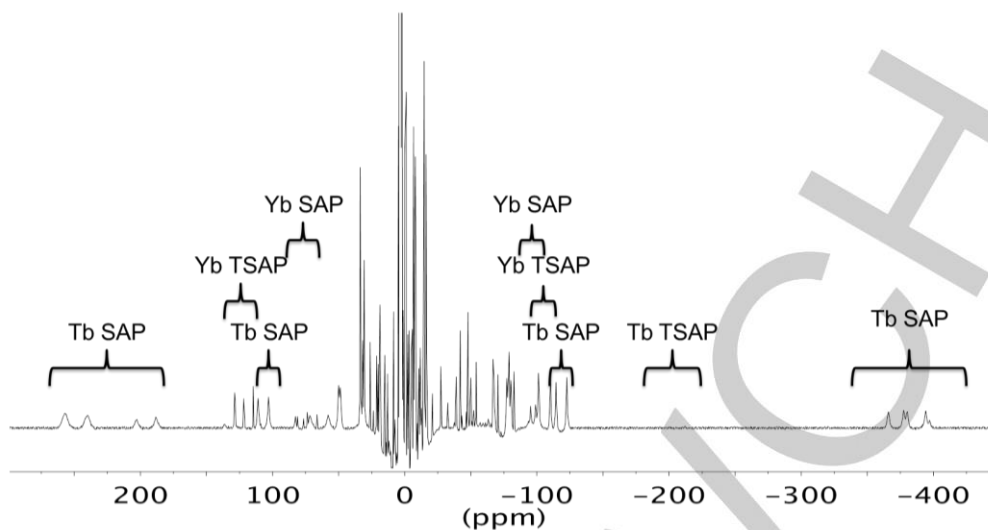


Figure 2. Paramagnetic ^1H NMR spectrum of EuTbYb.1

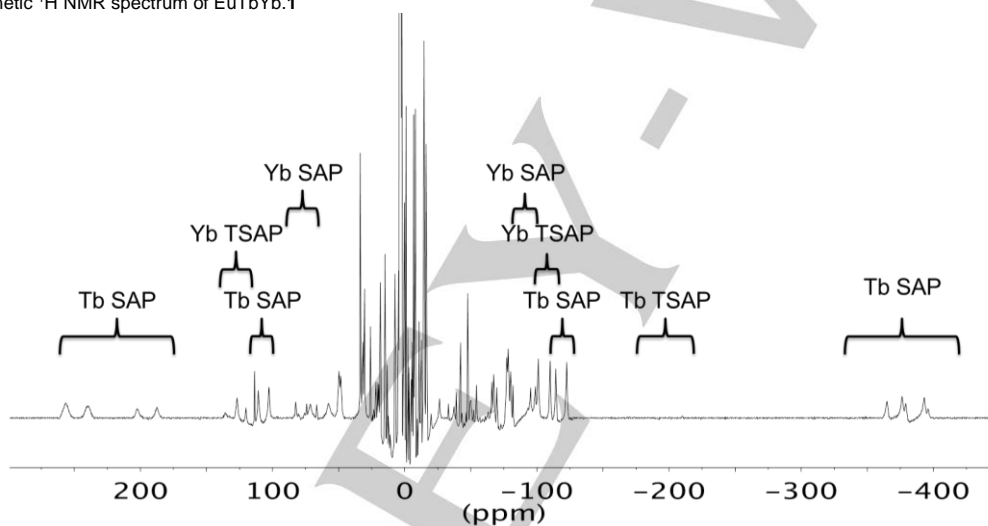


Figure 3. Paramagnetic ^1H NMR spectrum of EuTbYb.2.

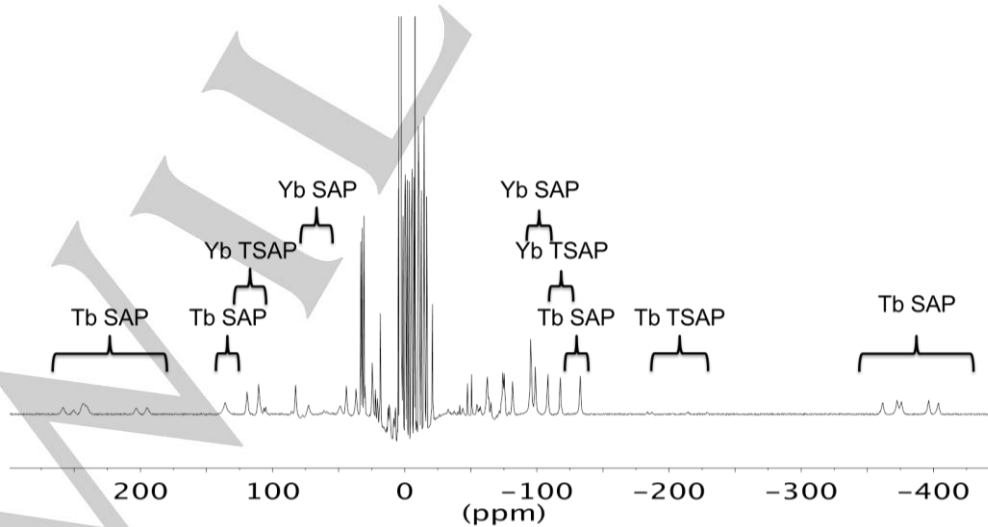


Figure 4. Paramagnetic ^1H NMR spectrum of TbEuYb.1.

Table 1. Lifetimes of the emission from the terbium, europium and ytterbium centre of TbEuYb.1, EuTbYb.1, and EuTbYb.2 in H₂O and D₂O. From the lifetimes, τ , the number of inner sphere solvent molecules, q , was calculated. N is the number of independent determinations, \pm is the standard deviation is given.

		EuTbYb.1		EuTbYb.2		TbEuYb.1	
		D ₂ O	H ₂ O	D ₂ O	H ₂ O	D ₂ O	H ₂ O
Yb	N	4	4	4	4	3	4
	$\tau^{[a]} / \mu s$	6.48	1.43	6.83	1.55	6.69	1.35
	\pm	0.20	0.10	0.41	0.09	0.08	0.07
	$q^{[b]}$	0.3(4) \pm 0.03		0.3(0) \pm 0.17		0.3(9) \pm 0.04	
Tb	N	4	4	4	5	3	5
	$\tau^{[c]} / ms$	1.45	1.47	2.30	1.65	1.45	1.45
	\pm	0.04	0.05	0.07	0.07	0.02	0.04
	$q^{[b]}$	-0.3(5) \pm 0.1 ^[d]		0.5(6) \pm 0.06		-0.3(0) \pm 0.05	
Eu	N	6	5	7	5	4	4
	$\tau^{[c]} / ms$	1.08	0.58	1.35	0.57	1.52	0.61
	\pm	0.08	0.03	0.08	0.03	0.08	0.02
	$q^{[b]}$	0.6(7) \pm 0.04		0.9(4) \pm 0.06		0.8(9) \pm 0.02	

[a] Lifetime determined from a deconvolution fit, each lifetime is determined from 4 measurements across the ytterbium emission band. [b] Number of inner sphere solvent molecules calculated using the equation: $q = A(k(H_2O) - k(D_2O) - B)$, where $k = 1/\tau$. A and B are $1 \mu s^{-1}/0.20 \mu s^{-1}$, $5 ms^{-1}/0.06 ms^{-1}$ and $1.2 ms^{-1}/0.25 ms^{-1}$ for Yb, Tb, and Eu respectively. [c] Lifetimes determined from a single exponential fit to the time-resolved emission profile. The europium lifetime was determined from emission at 700 nm and 615 nm following excitation at 392 nm and 300 nm. The terbium lifetime was determined from emission at 545 nm and 488 nm following excitation at 488 nm and 300 nm. [d] The negative q values indicate that there exist an excited state equilibrium involving terbium and naphthalene centred excited states.

Extrapolating from the resonances observed for terbium in TbEuYb.1, and EuTbYb.1 we must assume that the europium and terbium binding pockets are predominately in the square antiprismatic (SAP) conformation, with a minor contribution of the twisted square antiprismatic isomer (TSAP). The conformation of the ytterbium binding pocket on the other hand is found to be exclusively TSAP.

The luminescence spectra of TbEuYb.1, EuTbYb.1, and EuTbYb.2 show emission lines corresponding to the three lanthanide(III) ions following either direct or sensitized excitation. Time-resolved emission profiles were recorded in H₂O and D₂O

and fitted using a mono-exponential decay model. Several measurements (N) were performed to determine the experimental error in the lifetime (τ) determination. The results of the time-resolved luminescence experiments are compiled in Table 1. Determining τ in H₂O and D₂O allows for the calculation of lanthanide bound solvent molecules (q) using the modified Horrocks' equation.⁴⁴ The equation is not reliable if other major pathways for de-activation of the lanthanide excited state, such as energy back transfer to a chromophore, are accessible.⁴² This is the case in LnLn'Yb.1 where the reversible energy transfer between terbium and naphthalene makes q irrelevant for terbium.³⁶ For europium and ytterbium, q allows for an analysis of the structure of the individual binding pocket. As q_{Eu} and q_{Yb} are essentially identical across the series of complexes studied here, it is fair to assume that the two DOTA monoamide binding pockets are identical and that the DO3A-triazolyl binding pocket is similar. The value of q is (as expected) around $q = 1$ for europium and terbium (assuming the values from EuTbYb.2 are representative for terbium), and around $q = 0$ for the smaller ytterbium ion. Differences observed in the photophysical properties for the lanthanide(III) ions in TbEuYb.1, EuTbYb.1, and EuTbYb.2 must therefore relate to the interplay of the individual lanthanide(III) ions and the organic chromophores in the molecular structure.

Figure 5 shows the excitation spectra obtained while monitoring terbium and europium centred emission alongside the component absorption spectra. For terbium, direct excitation dominates in the formation of terbium centred excited states. In TbEuYb.1, a small contribution in the wavelength range around 300 nm can be assigned to sensitisation of terbium. The molecular structure must prevent energy transfer from the naphthalene group to terbium in EuTbYb.1, while energy transfer from the triazole to terbium does not occur. For europium, the triazole may act as a sensitizer and does so in EuTbYb.1, and EuTbYb.2. Direct excitation of europium does also occur in these two systems, and a small contribution following excitation of naphthalene can also be observed. In TbEuYb.1, europium excited states appear to be exclusively formed following direct excitation. The spectra presented in Figure 5 must imply that only the lanthanide(III) ion originating from Ln.3 in LnLn'Yb.1 and EuTbYb.2 can be sensitised by the two chromophores in the architectures.

While the sensitisation of terbium by naphthalene is only evident in the excitation spectrum of TbEuYb.1, the negative q_{Tb} values (table 1) show that the reverse energy transfer process occurs in both TbEuYb.1 and EuTbYb.1. This observation can be rationalised by the difference in the lifetime of the two donor states, where the naphthalene states exists in μs , while the terbium centred excited state is populated in multiple ms. The energy transfer mechanism is electron exchange (Dexter), which requires orbital overlap. Improbable conformations in TbEuYb.1 and EuTbYb.1 are needed for the energy transfer to occur. Therefore the lifetime of the donor state becomes important. Note that the conformations where energy transfer between terbium and naphthalene does occur must be visited more often in TbEuYb.1 as naphthalene does act as a sensitizer for terbium centred emission in this system (Figure 5).

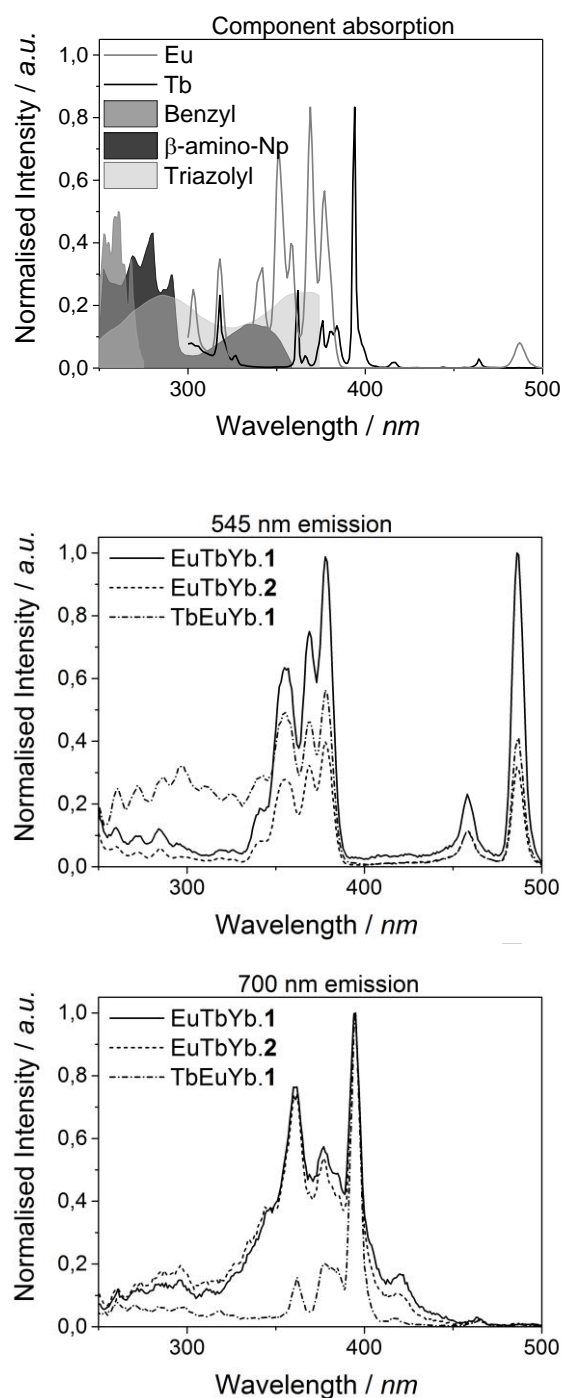


Figure 5. Absorption and excitation spectra of the ligand chromophores and naked lanthanide(III) ions in solution, and luminescence excitation spectra of TbEuYb.1, EuTbYb.1, and EuTbYb.2 in D₂O recorded monitoring terbium centred emission (545 nm, top) and europium centred emission (700 nm, bottom).

The differences induced by the relative position of chromophores and lanthanide(III) centres in the excited energy transfer cascades illustrated by the data in figure 5 and Table 1

are confirmed by the emission spectra shown in Figure 6. Excitation in the organic chromophores at 300 nm, where absorption by naphthalene dominates, gives rise to predominantly terbium centred emission in TbEuYb.1, while europium centred emission dominates when the two ions exchange position. Excitation at 392 nm, primarily direct excitation of europium, leads to very similar spectra, while direct excitation of terbium at 488 nm leads to identical spectra. These results confirm the assumption that the lanthanide(III) binding pockets are very similar.

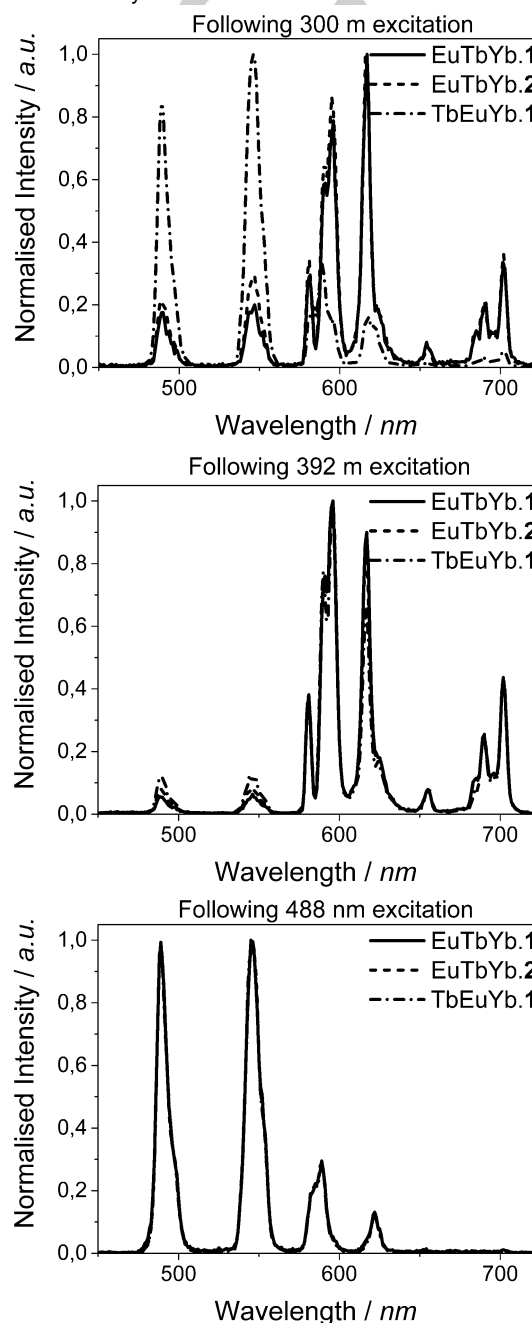
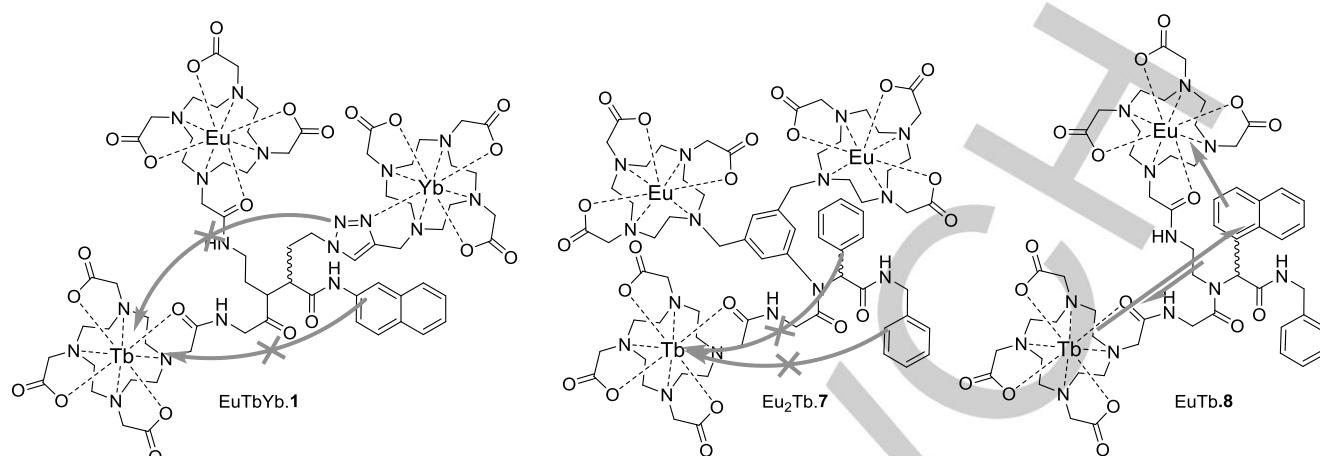


Figure 6. Luminescence emission spectra of TbEuYb.1, EuTbYb.1, and EuTbYb.2 in D₂O recorded following excitation at 300 nm (top), 392 nm (centre), and 488 nm (bottom).



Scheme 4. Multiheterometallic lanthanide(III) ion containing architectures, grey arrows indicate energy transfer processes.

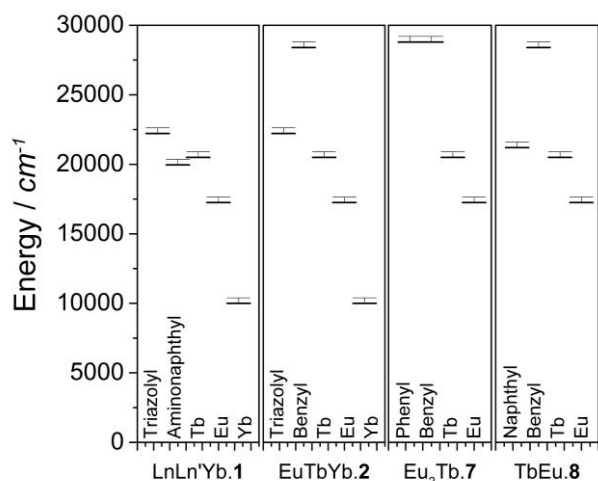


Figure 7. Relative energy levels of chromophores and lanthanide(III) centres in multiheterometallic lanthanide architectures **1**, **2**, **7**, and **8**.^{32, 56}

Having investigated the photophysical properties of **1** and **2**, we are able to conclude that energetics alone does not determine the properties of the studied systems. The conformation of the molecule must play an important role. Figure 7 shows the energy levels of the chromophores in the architectures and the lanthanide(III) ions. Figure 7 includes two other architectures that have been investigated previously, see scheme 4.^{34, 36, 42} Considering just the energy level diagrams, terbium should not be emissive in LnLnYb.1, while the ytterbium centre should be the end point of all energy transfer cascades. The results clearly contradict these assumptions. Clearly, the main reason that this is not the case lies in the rates of energy transfer between the different chromophores and lanthanide(III)

ions. The rate of energy transfer is not solely determined by relative energies, but also by ligand (and complex) structure, donor-acceptor separation, and (in the case of Förster mechanisms) spectral overlap. The effectiveness of the Förster mechanism is limited by the sharp absorption lines and ineffective overlap with the donor chromophores, meaning that Dexter exchange mechanisms are likely to dominate if they are feasible.

However, the strict requirements of Dexter energy transfer (direct contact between donor and acceptor) can be challenging to meet in larger architectures, where conformational change can potentially govern the prospects for superexchange pathways. In the complicated solution structure of kinetically inert lanthanide(III) complexes, the structural complexity is taken to the extreme in the large architectures shown in scheme 4. Thus by scrutinizing the photophysical properties of these, we are able to probe the solution structure of these molecules.

Energy transfer that does not occur despite favourable energetics must be prohibited by the simple fact that the two parts of the molecule—where the donor and acceptor states are localise—never are sufficiently close to one another to permit electron exchange (whose probability varies with the separation r as e^{-r}). That is, the solution structure prohibits the occurrence of an otherwise favourable energy transfer.

By considering kinetics, we can go a step further. The chromophore centred excited states have a limited lifetime, thus rarity of intramolecular collisions may be sufficient to block a favourable energy transfer. On the other hand, if no back energy transfer from a lanthanide(III) ion occurs, the millisecond lifetime of the lanthanide(III) centred excited state essentially dictates that intramolecular collision between chromophore and the lanthanide(III) centre does not take place in the architecture. Therefore, knowledge of the solution structure of lanthanide(III) complexes is crucial when designing architectures aimed at exploiting the unique properties of these ions.³⁶

These observations build upon our earlier discovery that, in EuTb.8 and TbEu.8, the intensities of emission from the

lanthanide(III) centres are determined by the relative positions of the lanthanide(III) centres to the naphthalene chromophore, which makes one of the two complexes a vastly superior ratiometric probe for oxygen.³⁶ The various possibilities for energy transfer in a range of systems are shown in scheme 4. It suggests that energy transfer is an effective probe of solution structure in molecular architectures containing several different lanthanide(III) ions

Conclusions

Three trinuclear triheterometallic lanthanide architectures were prepared using kinetically inert lanthanide(III) complexes as building blocks. The architectures were characterized using NMR and luminescence spectroscopies. The energy transfer from the chromophores in the structure to the lanthanide(III) centres highlighted the importance of understanding the solution structure of lanthanide(III) complexes, when designing functional probes based on the unique properties of lanthanide(III) ions. For the investigated compounds we can conclude that the spatial arrangement of the chromophores and lanthanide(III) centres prohibits the intramolecular collisions required for efficient Dexter energy transfer between sensitizing chromophore and lanthanide(III) centres. We advocate that steric congestion must be considered when designing lanthanide(III) based luminescent materials.

Experimental Section

All emission spectra were recorded using a Horiba Fluorolog-3 in phosphorescence mode in a 1 cm square quartz cuvette. The emission from the triazolyl moiety overlaps the terbium and europium centred emission and precludes the use of fluorescence mode. The parameters for spectra acquisition is identical for all spectra with a delay time of 0.1 ms and a sample window of 3 ms. The active monochromator had a slit of 5 nm and the passive monochromator had a slit of 14 nm. Emission spectra were recorded with excitation at 300 nm, 392 nm and 488 nm. Excitation spectra were recorded with emission at 545 nm, 590 nm and 700 nm. The absorption spectra were run on a single beam spectrometer using dark and baseline correction. The spectral resolution was determined by applying a 1 nm slit. Ytterbium lifetimes were measured following excitation using a nitrogen discharge laser (PTI-3301, 337nm) or a nitrogen pumped dye laser (PTI-330, 366 nm, 520nm), operating at 10Hz. Light emitted right angles to the excitation beam was focused onto the slits of a monochromator (PTI120), which was used to select the appropriate wavelength. The growth and decay of the luminescence at selected wavelengths was detected using a germanium photodiode (Edinburgh Instruments, EI-P) and recorded using a digital oscilloscope (Tektronix TDS220) before being transferred to a PC for analysis. Lifetimes were obtained by iterative reconvolution of the detector response with exponential components for the growth and decay of the lanthanide luminescence, using an approach described previously.⁵⁷

Molecular models were investigated using the Spartan'08 software package. A conformational search was performed in vacuo using semi-empirical methods (PM3) on the gadolinium complex.

NMR spectra of samples in D₂O at 298K were recorded at 700 MHz on a Varian VNMRs-700 using pre-saturation of the residual water signal.

Mass spectrometry analysis performed using ESI-QP and MALDI-TOF with DHB, DCTB, CHCA and THAP matrices. Sample also analysed by NESI-FTMS in MeOH(10% NH₄ OAc), MeOH(10% HCO₂ H), and MeOH(10% AcOH) solvent systems and MALDI-FTMS. No ions corresponding to starting materials was observed.

All chemicals and materials were used as received. The starting materials: Ln.3,⁵⁵ Ln.4,³⁴ Yb.5²⁹ and Yb.6³³ were prepared as previously reported. The Ugi coupling was performed using the method previously reported,^{33, 34, 52} a general procedure is given below.

General synthetic procedure to make Ugi-coupled architectures:

The amine appended complex Ln.3 (9 µmol) was added to a solution containing the carboxylate appended complex Ln.4. (11 µmol), either benzyl or 2-naphthyl isocyanide (11 µmol), the aldehyde appended ytterbium complex (Yb.5) (11 µmol), and Na₂SO₄ (0.132 g, 0.9 mmol) in ethanol (5 mL). The reaction mixture was stirred at room temperature for 6 days. The solids were removed by filtration and the filtrate evaporated. The crude product was washed with diethyl ether (5 x 20 mL), redissolved in methanol and precipitated by addition of diethyl ether to give an off-white solid. The product was purified by dialysis using a 1000 Da membrane. The water was changed every 12 hours for 4 days. After removal of the solvent the product was obtained as an off-white hygroscopic powder.

The composition of the complexes was verified using paramagnetic NMR and luminescence spectroscopy. Mass spectrometry did not reveal the ions corresponding to starting materials. The products could not be observed using any of the common forms of ionisation available in Oxford, Swansea, and Copenhagen.

Acknowledgements

The authors are grateful for support from the Universities of Oxford and Durham, the Danish Council for Independent Research, the Carlsberg Foundation, Christ Church, and Keble College for financial support.

Keywords: Lanthanides • Luminescence • Solution Structure • Molecular Building Blocks • Synthesis design

- [1] P. Caravan, J. J. Ellison, T. J. McMurphy, R. B. Lauffer *Chemical Reviews*. **1999**, 99, 2293-2352.
- [2] A. D. Sherry, P. Caravan, R. E. Lenkinski *Journal of Magnetic Resonance Imaging*. **2009**, 30, 1240-1248.
- [3] A. Datta, K. N. Raymond *Acc Chem Res*. **2009**, 42, 938-947.
- [4] J. L. Major, T. J. Meade *Acc Chem Res*. **2009**, 42, 893-903.
- [5] P. Caravan *Acc Chem Res*. **2009**, 42, 851-862.
- [6] S. Faulkner, O. A. Blackburn in *The Chemistry of Lanthanide MRI Contrast Agents*, Vol., John Wiley & Sons, Inc, **2014**, pp.179-197.
- [7] M. Polasek, P. Caravan *Inorganic chemistry*. **2013**, 52, 4084-4096.
- [8] E. M. Gale, I. P. Atanasova, F. Blasi, I. Ay, P. Caravan *Journal of the American Chemical Society*. **2015**, 137, 15548-15557.
- [9] S. Aime, M. Fasano, E. Terreno *Chemical Society reviews*. **1998**, 27, 19.
- [10] A. D. Sherry, J. Ren, J. Huskens, E. Brucher, E. Toth, C. F. C. G. Geraldes, M. M. C. A. Castro, W. P. Cacheris *Inorganic chemistry*. **1996**, 35, 4604-4612.

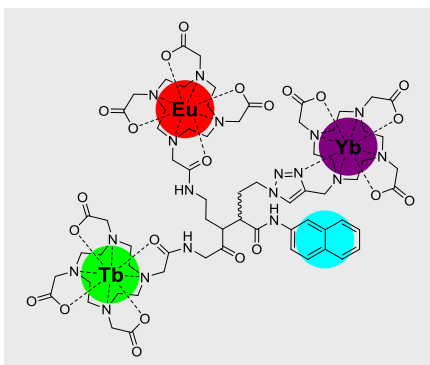
- [11] M. Woods, Z. Kovacs, R. Király, E. Brucher, S. Zhang, A. D. Sherry *Inorganic chemistry*. **2004**, *43*, 2845–2851.
- [12] G. Tircsó, Z. Kovács, A. D. Sherry *Inorganic chemistry*. **2006**, *45*, 9269–9280.
- [13] F. K. Kálmán, Z. Baranyai, I. Tóth, I. Bányai, R. Király, E. Brucher, S. Aime, X. Sun, A. D. Sherry, Z. Kovács *Inorganic chemistry*. **2008**, *47*, 3851–3862.
- [14] Z. Baranyai, I. Bányai, E. Brucher, R. Király, E. Terreno *European Journal of Inorganic Chemistry*. **2007**, *2007*, 3639–3645.
- [15] A. Takacs, R. Napolitano, M. Purgel, A. C. Benyei, L. Zekany, E. Brucher, I. Toth, Z. Baranyai, S. Aime *Inorganic chemistry*. **2014**.
- [16] S. Aime, M. Botta, Z. Garda, B. E. Kucera, G. Tircso, V. G. Young, M. Woods *Inorganic chemistry*. **2011**, *50*, 7955–7965.
- [17] M. K. Thompson, M. Botta, G. Nicolle, L. Helm, S. Aime, A. E. Merbach, K. N. Raymond *Journal of the American Chemical Society*. **2003**, *125*, 14274–14275.
- [18] P. Caravan, C. Comuzzi, W. Crooks, T. J. McMurphy, G. R. Choppin, S. R. Woulfe *Inorganic chemistry*. **2001**, *40*, 2170–2176.
- [19] P. Baía, J. P. André, C. F. G. C. Geraldes, J. A. Martins, A. E. Merbach, É. Tóth *European Journal of Inorganic Chemistry*. **2005**, *2005*, 2110–2119.
- [20] E. Toth, E. Brucher, I. Lazar, I. Toth *Inorganic chemistry*. **1994**, *33*, 4070–4076.
- [21] A. Rodriguez-Rodriguez, D. Esteban-Gomez, R. Tripier, G. Tircso, Z. Garda, I. Toth, A. de Blas, T. Rodriguez-Blas, C. Platas-Iglesias *Journal of the American Chemical Society*. **2014**, *136*, 17954–17957.
- [22] F. K. Kalman, A. Vegh, M. Regueiro-Figueroa, E. Toth, C. Platas-Iglesias, G. Tircso *Inorganic chemistry*. **2015**, *54*, 2345–2356.
- [23] A. Pasha, G. Tircso, E. T. Benyo, E. Brucher, A. D. Sherry *Eur J Inorg Chem*. **2007**, *2007*, 4340–4349.
- [24] L. Burai, R. Király, I. Lázár, E. Brucher *European Journal of Inorganic Chemistry*. **2001**, *2001*, 813–820.
- [25] É. Tóth, R. Király, J. Platzek, B. Radüchel, E. Brucher *Inorganica Chimica Acta*. **1996**, *249*, 191–199.
- [26] A. Pasha, M. Lin, G. Tircsó, C. L. Rostollan, M. Woods, G. E. Kiefer, A. D. Sherry, X. Sun *JBC Journal of Biological Inorganic Chemistry*. **2008**, *14*, 421–438.
- [27] P. Táboršký, P. Lubal, J. Havel, J. Kotek, P. Hermann, I. Lukeš *Collection of Czechoslovak Chemical Communications*. **2005**, *70*, 1909–1942.
- [28] J. C. Weinreb, A. K. Abu-Alfa *Journal of Magnetic Resonance Imaging*. **2009**, *30*, 1236–1239.
- [29] M. Jauregui, W. S. Perry, C. Allain, L. R. Vidler, M. C. Willis, A. M. Kenwright, J. S. Snaith, G. J. Stasiuk, M. P. Lowe, S. Faulkner *Dalton transactions*. **2009**, 6283–6285.
- [30] M. P. Placidi, A. J. L. Villaraza, L. S. Natrajan, D. Sykes, A. M. Kenwright, S. Faulkner *Journal of the American Chemical Society*. **2009**, *131*, 9916–9917.
- [31] A. M. Nonat, C. Allain, S. Faulkner, T. Gunnlaugsson *Inorganic chemistry*. **2010**, *49*, 8449–8456.
- [32] M. Tropiano, N. L. Kilah, M. Morten, H. Rahman, J. J. Davis, P. D. Beer, S. Faulkner *J. Am. Chem. Soc.* **2011**, *133*, 11847–11849.
- [33] T. J. Sørensen, M. Tropiano, O. A. Blackburn, J. A. Tilney, A. M. Kenwright, S. Faulkner *Chem Commun (Camb)*. **2013**, *49*, 783–785.
- [34] M. Tropiano, O. A. Blackburn, J. A. Tilney, L. R. Hill, M. P. Placidi, R. J. Aarons, D. Sykes, M. W. Jones, A. M. Kenwright, J. S. Snaith, T. J. Sørensen, S. Faulkner *Chem Eur J*. **2013**, *19*, 16566–16571.
- [35] M. Tropiano, S. Faulkner *Chem Commun (Camb)*. **2014**, *50*, 4696–4698.
- [36] T. J. Sørensen, A. M. Kenwright, S. Faulkner *Chemical Science*. **2015**, *6*, 2054–2059.
- [37] M. Tropiano, A. M. Kenwright, S. Faulkner *Chemistry*. **2015**, *21*, 5697–5699.
- [38] T. Koullourou, L. S. Natrajan, H. Bhavsar, S. J. Pope, J. Feng, J. Narvainen, R. Shaw, E. Scales, R. Kauppinen, A. M. Kenwright, S. Faulkner *Journal of the American Chemical Society*. **2008**, *130*, 2178–2179.
- [39] E. Debroye, T. N. Parac-Vogt *Chemical Society reviews*. **2014**, *43*, 8178–8192.
- [40] A. Watkis, R. Hueting, T. J. Sorensen, M. Tropiano, S. Faulkner *Chemical Communications*. **2015**, *51*, 15633–15636.
- [41] R. Hueting, M. Tropiano, S. Faulkner *RSC Adv*. **2014**, *4*, 44162–44165.
- [42] M. Tropiano, O. A. Blackburn, J. A. Tilney, L. R. Hill, T. Just Sørensen, S. Faulkner *Journal of Luminescence*. **2015**, *167*, 296–304.
- [43] O. A. Blackburn, R. M. Edkins, S. Faulkner, A. M. Kenwright, D. Parker, N. J. Rogers, S. Shuvaev *Dalton transactions*. **2016**.
- [44] A. Beeby, I. M. Clarkson, R. S. Dickens, S. Faulkner, D. Parker, L. Royle, A. S. de Sousa, J. A. G. Williams, M. Woods *Journal of the Chemical Society, Perkin Transactions 2*. **1999**, 493–504.
- [45] K. J. Miller, A. A. Saherwala, B. C. Webber, Y. Wu, A. D. Sherry, M. Woods *Inorganic chemistry*. **2010**, *49*, 8662–8664.
- [46] G. Tircso, B. C. Webber, B. E. Kucera, V. G. Young, M. Woods *Inorganic chemistry*. **2011**, *50*, 7966–7979.
- [47] S. Aime, M. Botta *Inorganic chemistry*. **1990**, *177*, 101–105.
- [48] S. Aime, M. Botta, G. Ermondi *Inorg. Chem.* **1992**, *31*, 4291–4299.
- [49] O. A. Blackburn, J. D. Routledge, L. B. Jennings, N. H. Rees, A. M. Kenwright, P. D. Beer, S. Faulkner *Dalton transactions*. **2016**, *45*, 3070–3077.
- [50] O. A. Blackburn, A. M. Kenwright, P. D. Beer, S. Faulkner *Dalton transactions*. **2015**.
- [51] O. A. Blackburn, N. F. Chilton, K. Keller, C. E. Tait, W. K. Myers, E. J. McInnes, A. M. Kenwright, P. D. Beer, C. R. Timmel, S. Faulkner *Angewandte Chemie*. **2015**, *54*, 10783–10786.
- [52] M. Main, J. S. Snaith, M. M. Meloni, M. Jauregui, D. Sykes, S. Faulkner, A. M. Kenwright *Chem Commun (Camb)*. **2008**, 5212–5214.
- [53] L. S. Natrajan, A. J. Villaraza, A. M. Kenwright, S. Faulkner *Chem Commun (Camb)*. **2009**, 6020–6022.
- [54] S. J. Pope, B. J. Coe, S. Faulkner, E. V. Bichenkova, X. Yu, K. T. Douglas *Journal of the American Chemical Society*. **2004**, *126*, 9490–9491.
- [55] W. S. Perry, S. J. Pope, C. Allain, B. J. Coe, A. M. Kenwright, S. Faulkner *Dalton transactions*. **2010**, *39*, 10974–10983.
- [56] M. Montalti, A. Credi, L. Prodi, M. T. Gandolfi, Handbook of Photochemistry, CRC Press, Boca Raton, **2006**.
- [57] A. Beeby, S. Faulkner *Chem Phys Lett*. **1997**, *266*, 116–122.

Entry for the Table of Contents (Please choose one layout)

Layout 1:

FULL PAPER

We have made large distinct heteronuclear lanthanide architectures from kinetically inert building blocks. By combining optical and magnetic resonance spectroscopies, we are able to conclude that conformational freedom allowing for intramolecular collision is more important than apparent proximity for efficient energy transfer.



Thomas Just Sørensen,* Manuel Tropiano, Alan M. Kenwright, Stephen Faulkner*

Page No. – Page No.

Triheterometallic lanthanide complexes made from kinetically stable lanthanide building blocks

Additional Author information for the electronic version of the article.

Author: T. J. Sørensen	ORCID identifier 0000-0003-1491-5116
Author: S. Faulkner	ORCID identifier 0000-0003-1878-5857
Author: M. Tropiano	ORCID identifier
Author: A. M. Kenwright	ORCID identifier 0000-0002-7169-7103

WILEY-VCH
